Accepted manuscript version

Published on NDT & E International Volume 102, March 2019, Pages 137-143
https://doi.org/10.1016/j.ndteint.2018.11.012

Thermography is cool: defect detection using liquid nitrogen as a stimulus

Lei Lei[a,*], Giovanni Ferrarini[b], Alessandro Bortolin[b], Gianluca Cadelano[b], Paolo Bison[b], Xavier Maldague[a]

[a] *LVSN, University Laval, 1065 avenue de la Médecine, Québec (QC) G1V 0A6 Canada*
[b] *CNR-ITC, Corso Stati Uniti 4, 35127 Padova PD, Italy*

Abstract

This paper mainly explores cooling instead of heating for external stimulation in infrared thermography for NDT & E. Liquid nitrogen is sprinkled on the surface of a steel sample with flat-bottom holes and a thermal camera captures the whole process. Pulsed thermography and lock-in thermography are also employed to obtain a good comparison. In image processing procedure, the principal component thermography method is performed on all thermal images. Moreover, the corresponding receiver operating characteristic curves are established and discussed. A comparison of the results indicates that the liquid nitrogen technique could be considered as a valid option for NDT & E.

Keywords:
thermography, thermal imaging, FFT, experiment, defects

1. Introduction

In the Nondestructive Testing & Evaluation (NDT & E) field, active infrared (IR) thermography [1] is a technique widely used in assessing the conditions of parts of material components, with an extremely broad range of applications [2, 3]. Traditionally, Pulsed Thermography (PT) deploys a thermal stimulation pulse (flash or lamp heating) to produce a thermal contrast between the fea-

*Corresponding author
Email address: lei.lei.1@ulaval.ca (Lei Lei)

ture of interest and the background, then monitors the time evolution of the surface temperature by a thermal camera. With this rapidity and convenience, numerous studies have been devoted to this technique, that is now a standard procedure for thermal testing.[4, 5, 6, 7, 8, 9].

However, if the temperature of the material to inspect is already higher than the ambient temperature, it can be of interest to make use of a cold source such as a line of air jets (or water jets; sudden contact with ice, snow, etc.). In fact, it is possible to generate a thermal front on the specimen both with an hot or cold stimulus: what is important is the temperature differential between the thermal source and the specimen. An advantage of a cold source is that it does not induce spurious thermal reflections into the infrared camera as in the case of a hot thermal source. The main limitations of cold stimulation sources are related to practical considerations, as it is generally easier and more efficient to heat rather then to cool a part. Thus, the advantage and convenience of using the cold stimulation in active infrared thermography still remains to be investigated in detail and better understood. Using a cold source could extend the range of application of infrared thermography to cases where the specimen under analysis could not be heated, due to safety issues or physical reasons[10]. A cold source could be required while handling biological or organic materials that could not withstand a temperature increase, such as food. A cold stress is an usual procedure in medicine, for example to investigate the Raynaud's phenomenon [11]. The cold stress in medical application is favored also by its ability of triggering a reaction of the body under investigation [12]. Another field of investigation is the survey of concrete and composite materials in order to find cracks and delaminations due to the presence of water or ice. Also in this case, a cold source would significantly decrease the risk of altering the physical characteristics of the specimen. Nonetheless,in the past in the scientific community, only a limited number of studies investigating a cold approach (cooling as the external stimulation in active infrared thermography) have been performed on industrial product inspection[13, 14]. A study by Burleigh[15] showed that the cooling method with refrigerating liquids is feasible but requires caution to

ensure the safety. The work of (Lei et al.)[16] chose instead to use air cooling to survey refrigerated vehicles. All the available works do not give a quantitative information about the reliability of the cooling technique, especially in comparison with the traditional heating procedure.

Therefore, the aim of this paper is improving the current knowledge on cooling stimulation in infrared thermography. In order to perform a reliable comparison, three methods (two traditional techniques, pulsed thermography and lock-in thermography act as the reference) will be applied on a steel slab with different sizes of flat-bottom-holes. The thermographic images of the experiments will be treated to eventually produce a binary map of the location of the defects. This map will be statistically evaluated in terms of sensitivity and specificity[17] by comparison with the 'true' map of the defects, furnishing a rank of the three stimulation methods.

2. Experimental setup

One side stimulation approach is often used in the infrared thermography NDT & E field, which is also known as the reflection scheme: both the stimulation device and the camera stay on the same side of the sample being tested. This approach applied in reality is shown in Figure 1.

(a) Pulsed thermography set-up (b) Lock-in thermography set-up

Figure 1: Experimental set-up in the *reflection* mode

The following equipment was set up for this study:

- Infrared camera FLIR SC3000 (spatial resolution equal to 320×240 pixels, framerate up to 50Hz, QWIP sensor, spectral range 8-9 μm)
- Two pairs of flash lamps for a total of 10 kJ (electric) released in 5 ms
- One pair of modulated xenon lamps with 1kW each served as Lock-in stimulation
- An isolated bottle (500 ml) filled with liquid nitrogen.

2.1. Specimen

In this study, a steel specimen comprising flat-bottom holes of different depths and sizes will be examined. Their dimensions are depicted in Figure 2.

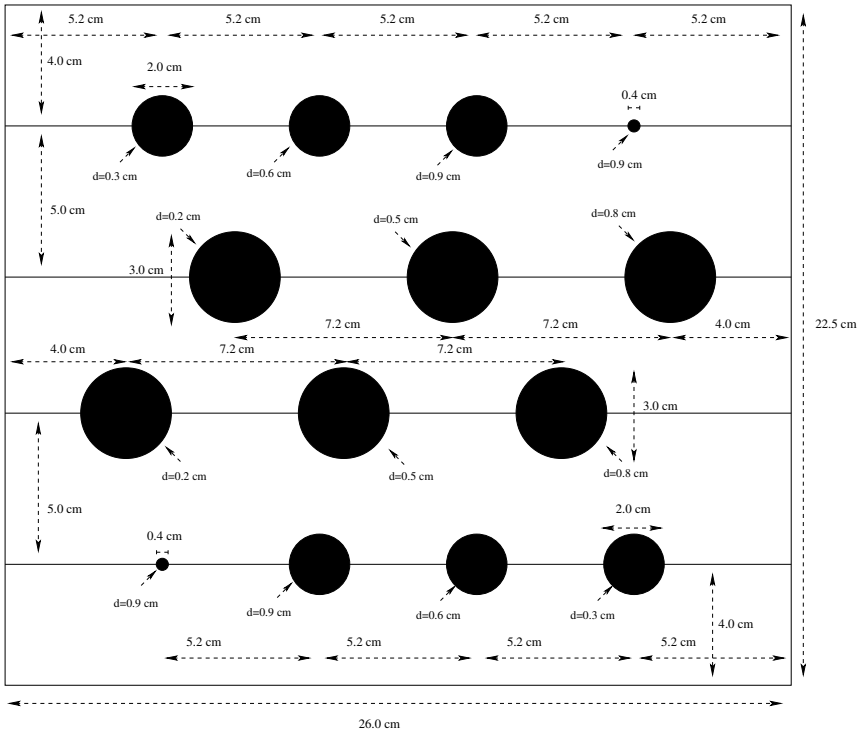

Figure 2: Steel sample dimension details with Flat-Bottom Holes of different depths and sizes (mirror image)

The steel plate has seventeen holes whose diameters vary from 0.4 cm to 3 cm, and whose depths (from bottom) vary from 0.3 cm to 0.9 cm. The entire

thickness is 1 cm. This specimen is painted before the test, in order to increase its emissivity and to obtain a homogeneous external stimulation.

2.2. Stimulation Techniques

Three external stimulations were deployed on the sample, for the sake of obtaining a good comparison in results:

- Pulse Thermography (PT)
- Lock-in Thermography (LIT)
- Liquid Nitrogen cooling (LN_2)

Known as the traditional and fast technique in NDT & E, pulse thermography (PT) acts as the reference during this test. One reason for this popularity is the quickness of the inspection relying on a thermal stimulation pulse, with duration going from a few ms for high thermal conductivity material inspection (such as metal specimen in this study) to a few seconds for low thermal conductivity specimens. Such quick thermal stimulation allows direct deployment on the plant floor with convenient heating sources.

Lock-in thermography (LIT) is based on the remote measurement of local harmonic heat transport on a specimen where a remote energy deposition is performed. In LIT the phase angle between remote optical energy deposition and resulting temperature modulation is sensitive to subsurface features or defect of the specimen.[18] Wave generation is for instance performed by periodically depositing heat on the specimen surface (e.g. through sine-modulated lamp heating) while the resulting oscillating temperature field in the stationary regime is remotely recorded through its thermal infrared emission.

In this study, 3 different frequencies of 0.0625 Hz (LIT16–one period is equivalent to 16 seconds), 0.125 Hz (LIT8–one period is equivalent to 8 seconds) and 0.25 Hz (LIT4–one period is equivalent to 4 seconds) are performed in Lock-in Thermography.

The liquid nitrogen LN_2 is applied in the test by means of pouring it out directly onto the surface in order to cool the sample. LN_2 was poured onto

the specimen center and allowed to spread out forwards the edges. The whole capture duration is 500 frames with 50 Hz of image frequency, ie. 10 seconds of recording. The pouring time (cooling time) is about 2 seconds, due to the bottle with a volume of 500 ml, with 100 frames in the results sequence. This way of cooling has a limit of that the central part will be first and mainly cooled, then the cold front propagates from center to the edges. This can lead to a drawback that in the final thermograms defects closer to the edges will be harder to detect. The flat surface of the samples helps the pouring process, that would be more difficult for irregular or concave surfaces. Performing the experiment in a laboratory with a control of temperature and humidity and checking the initial temperature of the specimen solves the possible issues related to condensation. The liquid nitrogen may produce some vapor on the inspected surface, but in practice they do not influence the inspection results aside from the fact that few early images could be discarded. This problem can be solved by providing a proper ventilation over the specimen after the pouring phase, but this poses some technical challenges that currently are difficult to address. In addition, as the traditional stimulation in Pulsed Thermography, the appearance of the defects is during the cooling down time, therefore, for cold stimulation, defects appear during the re-heating up time. For this reason, the initial thermograms (which contain nitrogen vapor, or even water vapor) were removed for post-processing.

3. Processing Methods

The following image-processing techniques and data-analysis methods were employed for this study:

- Principal Component Thermography (PCT)
- Phase and Amplitude images by Fast Fourier Transform (FFT)
- Receiver Operating Characteristic curves (ROC curves)

3.1. Principal Component Thermography (PCT)

The principal component thermography technique[19] uses Singular Value Decomposition (SVD) to reduce the matrix of observations to a highly compact statistical representation of the spatial and temporal variations relating to contrast information associated with underlying structural flaws".

3.2. FFT in Phase and Amplitude for LIT

In addition to the common technique for NDT & E, Fast Fourier Transform in LIT[18] is also one of the most applied techniques in infrared thermography, which is based on the periodic heating of the object being tested. A thermal wave is likewise generated and propagates inside the material. In real experimental cases the thermal wave is composed by a principal frequency and several harmonics where the amplitude of the Fast Fourier Transform is a function of frequency. The component corresponding to the principal frequency is selected to produce the amplitude and phase maps. By selecting the component with the highest amplitude it is possible to produce a phase map at the corresponding frequency where the defect appears enhanced.

3.3. ROC curve analysis

The post processing of experimental thermal data could be conducted in different ways in order to estimate the probability of a correct defect detection[20]. The Receiver Operating Characteristic (ROC) curve is a technique in statistics which helps visualize, organize and select classifiers based on their performance. The curve graph is created by plotting the True Positive Rate (TPR) against the False Positive Rate (FPR) at various threshold settings. More details about concepts and definitions can be found in [T. Fawcett 2006][17]. While being frequently chosen as a standard method in several scientific fields, ROC are rarely applied in the thermographic field[21].

Implemented in this study, a binary map of the defect locations is built and correlated to the post-processed images in gray scale. The main algorithm in the calculation of TPR and FPR is clarified as:

1. Choose the post-processed thermogram in which most defects shown as the test image;
2. Resize the defect map to the same size as that of the test image;
3. Choose a thresholding step number $N(N = 1000$ in this study) and establish the step value of thresholding [from 0, $\frac{1}{N}$, $\frac{2}{N}$ till $1(= \frac{N}{N})$];
4. For each thresholding step, binarize the test image with the thresholding and then compare it to the defect map, in order to obtain the corresponding TPR and FPR values;
5. Iterate the binarization and comparison so as to plot a whole curve.

4. Results & Discussion

Figure 3 illustrates the thermal raw images of PT and LN_2. The LIT FFT results can be found in figure 4.

4.1. Thermal images comparison

From the results above, raw images in figure 3 indicate that the most detectable flaws are the ones with a high aspect ratio (ie. diameter-to-depth). In addition, for the PT stimulation, a small hole with diameter 0.4 *cm*, depth[1] 0.9 *cm* (left-upper in figure 3(a)) appeared in frame 23, and disappeared after. Other holes, two with diameter 2 *cm* and depth 0.9 *cm*, and two with diameter 3 *cm* and depth 0.5 *cm*, (center in figure 3(b)) appeared in frame 60. Nonetheless, in LN_2 raw results, same defects as the one in Flash frame 60 appeared in LN_2 frame 41 (however, it should be noted that the first 100 frames of cooling time has been removed from these final raw images. The reason is because there was much noise from nitrogen gases in the thermal images). After this, there was no more defect that emerged. Another remark is that since the LN_2 is poured onto the center of the surface, there could be the situation that the center part

[1]It should be noted that the depth values mentioned here and after are from the bottom of the sample, therefore the real corresponding depths should be these values subtracted from the thickness.

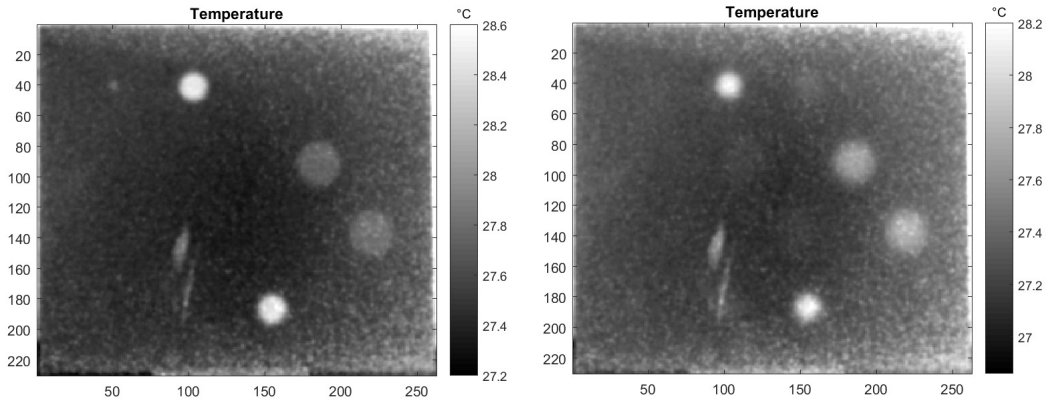

(a) Flash raw frame 23

(b) Flash raw frame 60

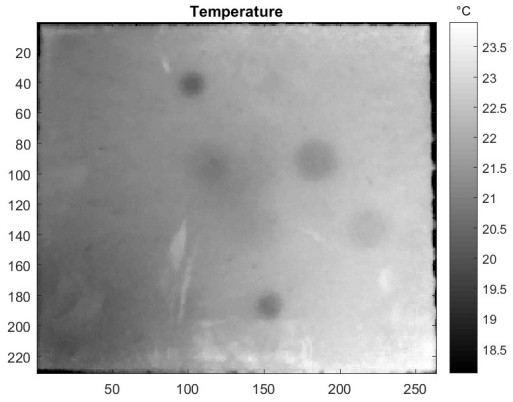

(c) LN_2 raw frame 41

Figure 3: Thermal raw images of PT and LN_2 stimulation techniques

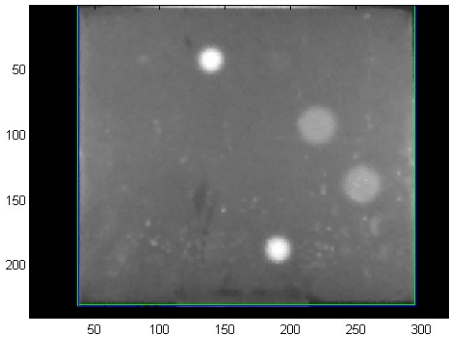

(a) LIT4 FFT in amplitude

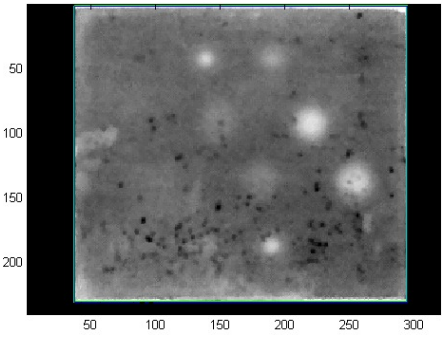

(b) LIT4 FFT in phase

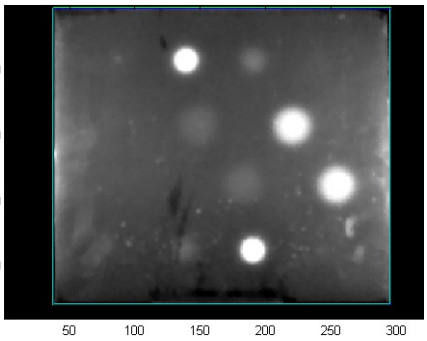

(c) LIT8 FFT in amplitude

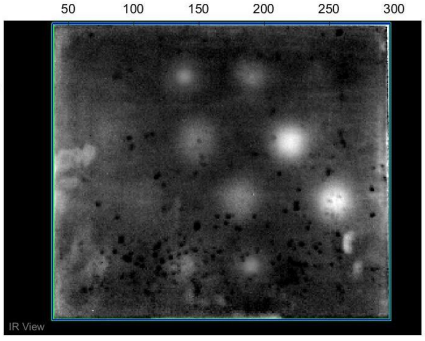

(d) LIT8 FFT in phase

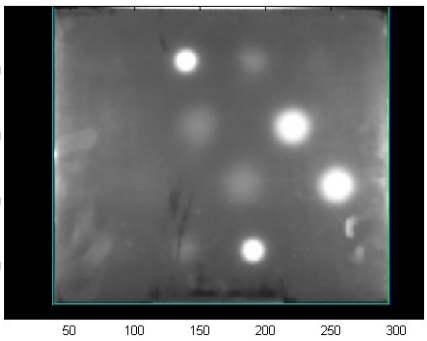

(e) LIT16 FFT in amplitude

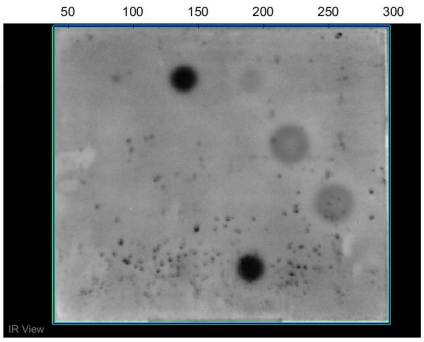

(f) LIT16 FFT in phase

Figure 4: FFT in amplitude and phase results for LIT

of specimen was over cooled while the 'cold front' (opposite to heat front) might have not be able to propagate to the edges. Due to the high conductivity of steel, defects only showed up at the beginning of the cooling procedure. These may be the main issues of pouring-out method.

For LIT results, FFT in amplitude has a better flaw detection capability than FFT in phase, as there is some noise in all of the phase images. LIT8 and LIT16 have about four more detected flaws than LIT4.

Following PCT processing, figure 5 exhibits a clearer result. It can be observed that most of the flaws are visible, especially in the Flash image (figure 5(a)). Less flaws are visible in the LIT4 PCT third image.

Comparing the processed thermal images, the following observations can be made:

- All techniques present part of the flaws in the sample;
- The PCT post-processing method displays a better results for all images;
- More defects are exhibited in Flash stimulation with PCT processing;

4.2. Corresponding ROC curves comparison

The ROC curves obtained from comparing the binary map of defect locations to the above results are represented in figure 6.

In the ROC curves definitions, the *sensitivity* is the True Positive Rate (*TPR*), and *1-specificity* is the False Positive Rate (*FPR*). From the curves of the PCT results (figure 6a), one can easily notice that the five curves have almost the same performance of classification in the beginning. When the *TPR* arrives at 0.3, the PT curve becomes the nearest to the northwest (where the *TPR* is higher, the *FPR* is lower or both). The second one is the LN_2 curve that has a slightly higher *TPR* than PT after the *FPR* reaches 0.4. The LIT8 and LIT16 curves have almost the same performance before the *TPR* attains 0.7. After that the LIT16 has a higher *TPR* than LIT8. The worst one is the LIT4 curve as it is the closest one to the diagonal line $y = x$, which represents the strategy of randomly guessing a class.

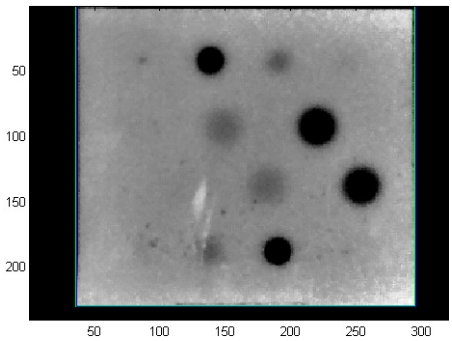

(a) Flash PCT 2nd Image

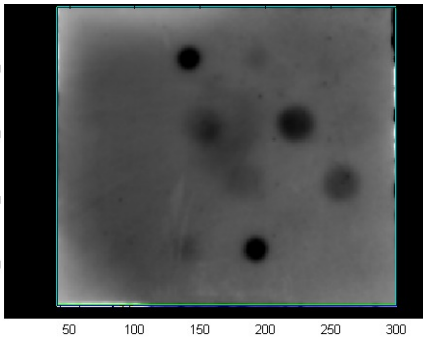

(b) LN_2 PCT 2nd Image

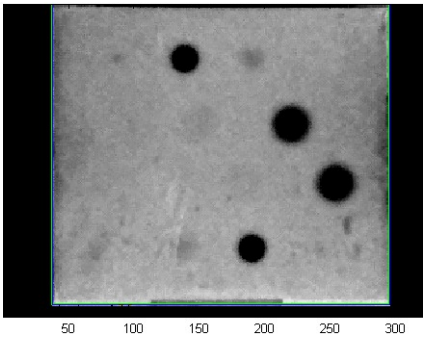

(c) LIT4 PCT 3rd Image

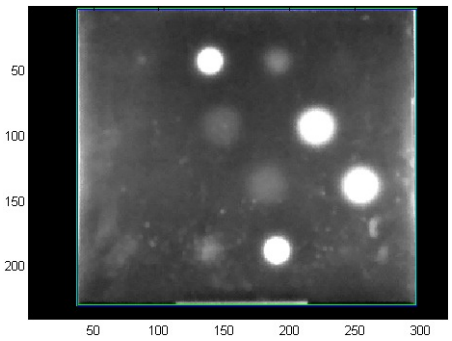

(d) LIT8 PCT 3rd Image

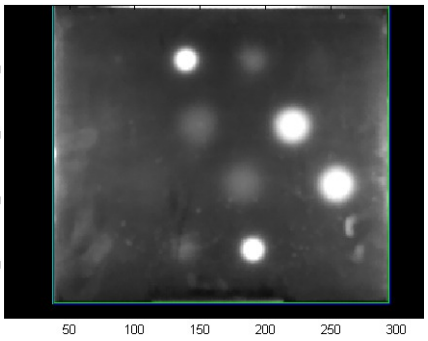

(e) LIT16 PCT 3rd Image

Figure 5: PCT results of corresponding technique

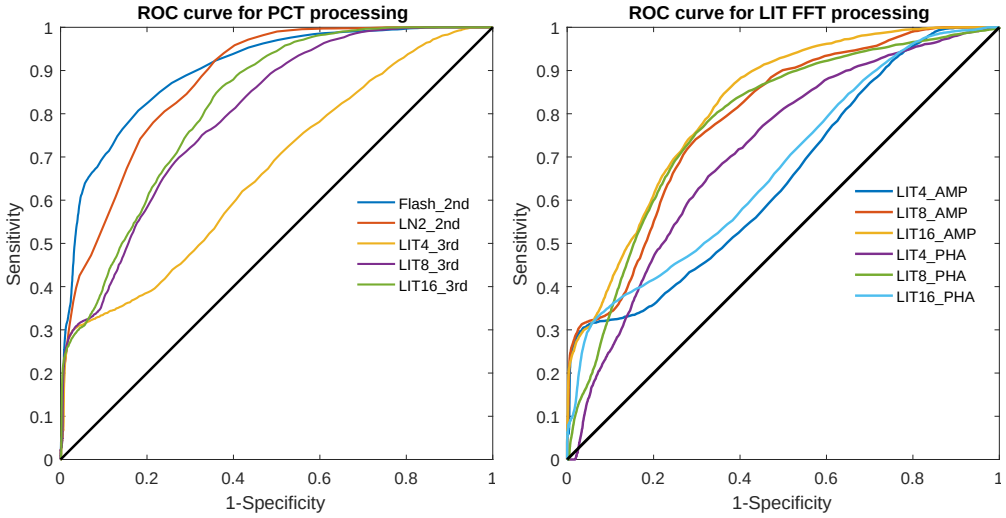

(a) ROC from PCT Results (b) ROC from LIT FFT results

Figure 6: ROC curves for PCT and FFT processing results

The situation is same for the curves obtained by LIT FFT results (Fig 6b), in which LIT4 in amplitude has an unfavorable performance in classification. This indicates again that 4 seconds of heating (LIT4) were not enough to penetrate the steel specimen deeply.On the other hand, for phase images, LIT8 has a better profile than LIT4 and LIT16, who have almost similar classification. In brief, for LIT FFT processing methods, FFT in amplitude has more favorable results than FFT in phase.

4.3. Area under curve analysis and comparison

In ROC analysis, a common method to compare different classifiers is to calculate the Area Under Curve (AUC) for each ROC curve[17]. In this way, a single scalar value will represent the expected performance of the classifiers. As in the ROC curve profile, the AUC is a part of the unit square area, therefore its value will be between 0 and 1. Thus, random guessing classifier produces a diagonal line between (0,0) and (1,1), which has an area of 0.5. It can be then indicated that a classifier AUC value less than 0.5 is even worse than a random guessing.

The corresponding AUC obtained from the above ROC curves is found in Tab. 1. Their comparison in form of the bar chart is illustrated in Fig. 7. A straight comparison shows that the Flash method with PCT second component has the highest AUC value of 0.9. The second one is the Liquid Nitrogen method, that is very close to the flash method with an AUC value of 0.87. At the bottom of the ranking, LIT4 with PCT third component and its amplitude one have the worst values as 0.67 and 0.65 respectively, which are just a bit better and a random guessing. On the contrary, LIT8 and LIT16 technique have a better result both in PCT processing and their FFT images. This might be caused by the fact that during one period, 4 seconds of heating (LIT4) were not enough to penetrate the steel specimen deeply as those of 8 seconds (LIT8) and 16 seconds (LIT16). On the other hand, all the Lock-in Thermography techniques have similar AUC value in their phase images, which indicates that for phase image results, heating time does not make an effective influence in Lock-in Thermography in this study. Considering all these results, though the best approach is pulsed thermography with PCT processing, the LN_2 technique can be considered as a valid alternative method

Method	**Value**
Flash-2nd	0.90
LN2-2nd	0.87
LIT4-3rd	0.67
LIT8-3rd	0.80
LIT16-3rd	0.82
LIT4-AMP	0.65
LIT8-AMP	0.79
LIT16-AMP	0.82
LIT4-PHA	0.71
LIT8-PHA	0.78
LIT16-PHA	0.67

Table 1: AUC value comparison

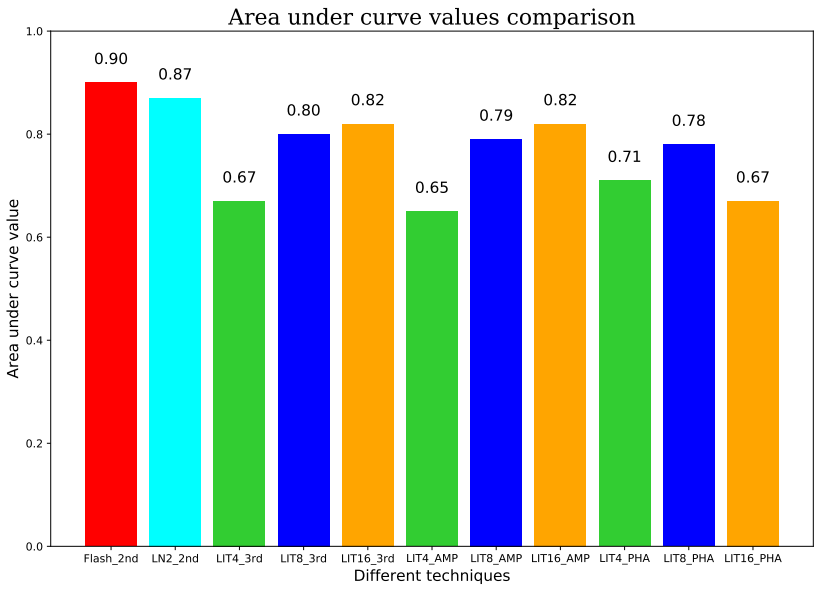

Figure 7: AUC value comparison

5. Conclusion

This study investigates an external stimulation–cooling instead of heating in infrared thermography for NDT & E. A steel specimen is used to test three different stimulations for thermal images and also ROC analysis comparison. Results shows that all techniques highlight part of the flaws in the sample, whereas the LN_2 technique represents the defects at the end of cooling process; this maybe due to the high conductivity of steel. In thermal results, the PCT post-processing method displays a better results for all procedures. More defects are exhibited in pulsed thermography with PCT processing. ROC curve analysis and its AUC analysis have elucidated a straightforward classification comparison, in which the best values are obtained with the pulsed thermography with PCT processing, trailed narrowly by the liquid nitrogen method.

The LN_2 technique should therefore be considered as a valid option for the survey of objects that should not be heated, such as biological tissues, organic

materials, dry or iced samples. With this purpose, future work will analyze different kinds of specimens. The method of liquid nitrogen pouring may be replaced by spraying onto the sample surface, which can reduce the inhomogeneous cooling problem. To enhance the penetration of heat inside the sample, a proposition involving heating on one side of the specimen and cooling the other side might be taken into consideration. The exploration of an opposite means of external stimulation in infrared thermography might favor new ideas for NDT & E.

ACKNOWLEDGMENTS

This research was supported by the governments of Italy and Quebec (Ministère des Relations internationales et de la Francophonie) through the Joint Subcommittee Québec-Italy, project n°08.0203. It was also supported by the Natural Sciences and Engineering Research Council of Canada (NSERC). We are also thankful to our collaborative institute CNR-ITC Padova which provided expertise that greatly helped in this research.

References

References

[1] X. Maldague, Theory and practice of infrared technology for nondestructive testing, Wiley, New York, 2001.

[2] V. P. Vavilov, Thermal nondestructive testing of materials and products: a review, Russian Journal of Nondestructive Testing 53 (10) (2017) 707–730. doi:https://doi.org/10.1134/S1061830917100072.

[3] G. Cadelano, A. Bortolin, G. Ferrarini, B. Molinas, D. Giantin, P. Zonta, P. Bison, Corrosion Detection in Pipelines Using Infrared Thermography: Experiments and Data Processing Methods, Journal of Nondestructive Evaluation 35 (3). doi:10.1007/s10921-016-0365-5.

[4] X. Maldague, Nondestructive Evaluation of Materials by Infrared Thermography, Springer-Verlag, London, 1993.

[5] X. Maldague, Infrared methodology and technology, Gordon and Breach, New York, 1994.

[6] C. Ibarra-Castanedo, M. Genest, S. Guibert, J. Piau, A. Maldague, X.and Bendada, Inspection of aerospace materials by pulsed thermography, lock-in thermography and vibrothermography: A comparative study, Thermosense XXIX, edited by Kathryn M. Knettel, Vladimir P. Vavilov, Jonathan J. Miles, Proc. of SPIE 6541 (2007) 654116–1. doi:https://doi.org/10.1117/12.720097.

[7] C. Ibarra-Castanedo, N. Avdelidis, E. Grinzato, P. Bison, S. Marinetti, C. Plescanu, A. Bendada, X. Maldague, Delamination detection and impact damage assessment of glare by active thermography, Int. J. Materials and Product Technology 41 (2011) 5–16. doi:https://doi.org/10.1504/IJMPT.2011.040282.

[8] Y. Duan, S. Huebner, U. Hassler, A. Osman, C. Ibarra-Castanedo, X. P. Maldague, Quantitative evaluation of optical lock-in and pulsed thermography for aluminum foam material, Infrared Physics & Technology 60 (2013) 275–280. doi:http://dx.doi.org/10.1016/j.infrared.2013.05.009.

[9] V. P. Vavilov, D. D. Burleigh, Review of pulsed thermal NDT: Physical principles, theory and data processing, NDT & E International 73 (2015) 28 – 52. doi:https://doi.org/10.1016/j.ndteint.2015.03.003.

[10] D. P. Livingston, T. D. Tuong, J. P. Murphy, L. V. Gusta, I. Willick, M. E. Wisniewski, High-definition infrared thermography of ice nucleation and propagation in wheat under natural frost conditions and controlled freezing, Planta 247 (4) (2018) 791–806. doi:10.1007/s00425-017-2823-4.

[11] A. Merla, L. Di Donato, S. Di Luzio, G. Farina, S. Pisarri, M. Proietti, F. Salsano, G. L. Romani, Infrared functional imaging applied to raynaud's

phenomenon, IEEE Engineering in Medicine and Biology Magazine 21 (6) (2002) 73–79. doi:10.1109/MEMB.2002.1175141.

[12] Y. Ohashi, I. Uchida, Applying dynamic thermography in the diagnosis of breast cancer: Techniques for improving sensitivity of breast thermography, IEEE Transactions on Biomedical Engineering 47 (6) (2000) 42–51. doi:10.1109/51.844379.

[13] H. Endoh, T. Hoshimiya, Dynamical observation of heat flow and the NDI in a simulated welded zone using active thermography with a coolant material, in: The 11 th International Conference on Quantitative InfraRed Thermography, Naples, Italia, 2012. doi:10.21611/qirt.2012.339.

[14] L. Hom, A. Durieux, J. Miler, M. Asheghi, K. Ramani, K. E. Goodson, Calibration methodology for interposing liquid coolants for infrared thermography of microprocessors, in: Thermal and Thermomechanical Phenomena in Electronic Systems (ITherm) and 2012 13th IEEE Intersociety Conference on, 2012, pp. 1412–1419. doi:10.1109/ITHERM.2012.6231585.

[15] D. Burleigh, Thermographic ndt of graphite epoxy filament-wound structures, Thermosense XI, Proc. of SPIE 1094 (1989) 175–181. doi:10.1117/12.953400.

[16] L. Lei, A. Bortolin, P. Bison, X. Maldague, Detection of insulation flaws and thermal bridges in insulated truck box panels, Quantitative InfraRed Thermography Journal (2017) 1–10doi:10.1080/17686733.2017.1336899.

[17] T. Fawcett, An introduction to roc analysis, Pattern recognition letters 27 (8) (2006) 861–874. doi:https://doi.org/10.1016/j.patrec.2005.10.010.

[18] D. Wu, G. Busse, Lock-in thermography for nondestructive evaluation of materials, Revue générale de thermique 37 (8) (1998) 693–703.

[19] N. Rajic, Principal component thermography, Tech. Rep. 1298, DTIC Document (2002).

[20] E. Grinzato, V. Vavilov, P. Bison, S. Marinetti, C. Bressan, Methodology of processing experimental data in transient thermal nondestructive testing (ndt), Proc.SPIE 2473 (1995) 2473 – 2473 – 12. doi:10.1117/12.204852.

[21] P. Bison, A. Bortolin, G. Cadelano, G. Ferrarini, L. Finesso, F. Lopez, X. Maldague, Evaluation of frescoes detachments by partial least square thermography, in: 12th International Conference on Quantitative Infrared Thermography, Bordeaux (France), 2014, pp. 07–11. doi:10.21611/qirt.2014.109.